

Annual Meeting Selection

Using 3D finite-difference modeling to design wide-azimuth surveys for improved subsalt imaging

Carl J. Regone¹

ABSTRACT

Three-dimensional finite-difference modeling studies conducted over subsalt structures in the deepwater Gulf of Mexico confirm the deficiencies of narrow-azimuth towed-streamer surveys and predict significant improvement in image quality with wide-azimuth methods. Finite-difference modeling has provided important design parameters for two separate approaches for wide-azimuth surveys: ocean-bottom receivers distributed in a sparse grid on the ocean floor coupled with a dense grid of source points on the surface, and a wide-azimuth towed-streamer method using multiple seismic vessels in a novel configuration. These two methods complement each other. Ocean-bottom receivers may be used effectively where field development has resulted in many obstacles that might interfere with towed-streamer methods, where the required size of the 3D survey is not too extensive, or where very long offsets are required for all azimuths. Towed-streamer methods are more efficient for large surveys, and key parameters in the wide-azimuth towed-streamer method can be varied to provide a wide range of cost versus data-quality options to make the method suitable for application in scenarios ranging from exploration to field development.

INTRODUCTION

Subsalt image quality in the deepwater Gulf of Mexico is often very poor with conventional narrow-azimuth towed-streamer (NATS) 3D seismic surveys, even when the most advanced processing and imaging methods available are used with great care. Failure to adequately suppress free-surface multiples and errors in the veloc-

ity model are often cited as the primary reasons for this. However, an earlier finite-difference (FD) modeling study comparing 3D acquisition geometries over a complex structure (Etgen and Regone, 1998) convinced me that the problem is primarily related to the narrow-azimuth acquisition geometry universally used with towed-streamer 3D seismic surveys and that there is a need to experiment with different acquisition geometries. Because the cost of such experimentation is prohibitive with real 3D surveys, we need an alternative method. One attractive method for providing the necessary range of experimental acquisition designs is 3D FD modeling.

In 3D FD modeling, we may use either the acoustic or elastic wave equation. Although 3D elastic FD modeling provides the most realistic simulations, there are several reasons why I choose to use acoustic modeling instead of elastic modeling. First, we generally have little knowledge of the shear velocities and absorption characteristics near the ocean floor. Because both of these have a large influence on the simulated data, this lack of knowledge detracts greatly from the desired realism. Second, with the computer technology available at the time of this study, the runtime for 3D elastic FD modeling is unacceptably long for these deepwater subsalt structures. Third, 2D elastic FD synthetics created over a cross section taken from the 3D structure studied in this paper show that events resulting from P-wave to S-wave conversions have a negligible effect on P-wave imaging of the subsalt structure and merely add a small amount of noise to the overall image.

Because the goal of this study is limited to subsalt structural imaging problems using P-waves, and such issues as anisotropy, S-wave imaging, and seismic attributes are not being considered, I believe that 3D acoustic FD modeling produces sufficiently realistic, full-scale simulations of the 3D seismic survey geometries being studied. One exception is the possibility that oceanbottom-receivers can be subject to undesired S-waves in the form of interface waves. As mentioned above, accurate modeling of these events requires knowledge of elastic properties near the ocean floor that we do not have. Conse-

Presented at the 76th Annual International Meeting, SEG. Manuscript received by the Editor August 7, 2006; revised manuscript received October 24, 2006; published online August 23, 2007.

¹BP America Inc., Houston, Texas. E-mail: regonecj@bp.com.
© 2007 Society of Exploration Geophysicists. All rights reserved.

quently, acoustic modeling of ocean-bottom receivers may not include all the problems that the real receivers may encounter.

The seismic traces resulting from 3D FD modeling may be processed as desired and the migrated image volumes may be carefully analyzed to determine differences in image quality. Because 3D FD synthetic data may be created with or without free-surface multiples, and because the exact velocity model is known, it is possible to isolate the effects of acquisition geometry on image quality. In this paper, I use 3D FD modeling to evaluate two different methods for acquiring wide-azimuth data: a wide-azimuth towed-streamer (WATS) method using multiple seismic vessels, and a method using ocean-bottom seismometer (OBS) nodes distributed in a sparse grid on the ocean floor coupled with a dense grid of source points on the surface.

Ocean-bottom cables and vertical cables have also been used successfully to acquire wide-azimuth ocean-bottom 3D seismic surveys. These methods are not considered here because of operational reasons. Ocean-bottom cables are very difficult, if not impossible, to deploy in the 2000-m water depths of the target area. Further, we fear that draping long cables over the rough escarpment present in much of the area will cause coupling problems. Vertical cables (Kraile, 1994) suffer from the strong currents present on the ocean floor in this area. These currents cause the cables to move during the time needed to record the 3D survey so that they are not vertical and are not consistently in the same location. These variable receiver locations are viewed as a fatal flaw for a common-receiver migration process.

The 3D FD modeling studies provided key design parameters for BP's successful efforts to acquire both WATS and OBS surveys. From late 2004 to early 2005, BP acquired a WATS survey at the Mad Dog field (Michell et al., 2006), and one year later, acquired an OBS survey at the Atlantis field (Beaudoin and Michell, 2006). In late 2006, BP commenced acquisition on additional WATS surveys for both field development and exploration purposes.

METHOD

For the deepwater, salt-related structures studied in this paper, 3D acoustic FD modeling is very compute intensive. The capability to execute such modeling at large scale is worth the cost, however, because it enables one to perform the controlled experiments needed to solve complex acquisition and imaging problems. Because model runtime is linear with computational model dimensions in x , y , and z and with the length of the seismic trace, the first step toward efficient FD modeling is to determine the minimum required sizes for each. The runtime is also proportional to the fourth power of the maximum frequency being modeled, so it is important to keep this frequency to the minimum value necessary to resolve the features built into the model. I use 2D FD modeling on cross sections extracted from the 3D model to estimate these parameters. For the 3D model described in this paper, these tests suggest 16×16 km computational models centered on the shot, 12-s trace lengths, and a maximum frequency of 15 Hz will be adequate.

Another important model parameter is shot density. A shot grid that is too coarse will result in unacceptable artifacts. One that is finer than necessary wastes computer resources. The optimum shot interval is related to both the structure and the frequency. I use 2.5D modeling to determine this parameter. A 2.5D model is one where there is no change in the geology in the strike direction. Therefore, a single line of 3D shots oriented in the dip direction is sufficient to permit the simulation of nearly any 3D survey geometry. Because

there is only one shot line, we can afford to use a small shot interval. Migrated images produced for various shot intervals may be used to determine the maximum interval for which artifacts are acceptable. For the model discussed in this paper, a 250-m shot interval in both the x and y directions is adequate. To compare acquisition geometries, I extract the appropriate subsets of sources and receivers, apply any trace processing desired, and then apply common-shot migration using an $\omega - x$ extrapolation method (Claerbout, 1970, 1976) and the exact velocity model.

Modeling OBS-nodes requires some special treatment. First, because the number of node locations is much smaller than the number of shots, reciprocity is used to swap sources and receivers. Second, processing OBS-node data with a free surface requires both a pressure component (p) and the vertical particle velocity (z component) to enable up/down wavefield separation for partial suppression of multiple reflections using P_z summation (Barr and Sanders, 1989; Amundsen and Reitan, 1995). Therefore, to model an OBS-node survey, we need to compute one pressure shot and one directional shot for each of the many thousands of node locations. The pressure shots are produced by our normal 3D acoustic FD code (Dablain, 1986; Holberg, 1987; Igel et al., 1995; Virieux, 1986). The directional shots are produced by a vector-acoustic algorithm capable of modeling multicomponent data (Etgen and O'Brien, 2007). These codes are high order (fourth-, eighth-, or twelfth-order in space and fourth-order in time), are run out-of-core, and compute single shots on individual machines. The processing of the OBS data consists of P_z summation for the receiver side multiples plus wavefield extrapolation for the source side multiples (Xia et al., 2006; Clarke et al., 2006) followed by common-shot migration.

Modeling towed-streamer and OBS-node data for both a free and an absorbing surface results in the need to produce many tens of thousands of FD shot records for each 3D model. To accomplish this in a timely manner, we use a dedicated modeling cluster consisting, at the time of this study, of 720 dual-processor Intel Xeon-based machines with 3.4 GHz clock frequencies and 4 Gbytes memory. The theoretical speed of the cluster is approximately 10 Tflops. With model parameters similar to those given above, we can compute 10,000 acoustic shots in about 20 days. With the vector-acoustic algorithm, z -component shots take about three to four times as long as the equivalent acoustic shots.

MODELING

The 3D FD modeling has shown that there are several important structure-dependent parameters affecting the data quality of both WATS and OBS surveys. The cost of acquisition is highly dependent on these parameter choices, and FD modeling is used to make informed decisions. For the OBS-node approach, these parameters include the total size of the node grid and its location relative to the geologic structure, the node spacing, and the extent of the source grid beyond the node patch. Parameter choices result in requirements for the number of nodes needed, the size of the node patch that can be deployed at one time, the number of these patches required for the entire survey, the total number of source points, and the length of time a node must be actively recording. For the Atlantis structure, where our first OBS-node field trial took place, these parameter choices led us to commission the construction of 900+ deepwater-capable nodes with a minimum 28-day battery life, to use a two-patch deployment and a total node grid size of approximately 16×16 km, to have a shot grid extending 7100 m outside the receiver

grid to the south and 4500 m to the north with minimum crossline offsets set to 6000 m, and to use a node spacing of approximately 400 m (Ross and Beaudoin, 2006).

For the WATS method, the key parameters are receiver patch dimensions, source location relative to the receiver patch, and sail-line separation. For the Mad Dog structure, where our first WATS field trial took place, the optimum parameters were an 8×4 km rectangular receiver patch with two source vessels located 8 km apart on the side of the receiver patch and a 250-m sail-line interval. This was achieved with one cable vessel pulling eight 8-km cables spaced 125 m apart and two source vessels. As shown in Figure 1, the receiver patch was divided into four 1-km-wide tiles, and each tile was an independently recorded 3D survey. For tile 1, the source vessels were as close as possible to the outermost cable, whereas for tile 4, the source vessels were 3 km from that cable (Threadgold et al., 2006). Details of the rationale behind this design may be found in (Regone, 2006). Essentially, I use a combination of reciprocity, dual source vessels to create a split spread, and 3D FD modeling to empirically determine the required shot density and receiver patch dimensions for the particular structure being studied. As the following figures show, the predicted improvement in data quality for both the WATS and OBS-node methods relative to standard NATS data is significant.

I use a 3D model of the Atlantis structure to compute both towed-streamer and OBS-node data. This structure is a four-way anticline, the northern half of which is located beneath a complex salt body and is very poorly imaged on existing NATS surveys. A complex, steep escarpment on the ocean floor located over the crest of the structure contributes to the imaging problems. The first step in the 3D FD modeling process is to build a scale model for velocity and density. The velocity model comes from a prestack depth migration project and, thus, contains discrete water and salt bodies. The sediment velocities are smoothly varying in the manner typical of tomographic velocity-analysis methods and are representative of a compaction model for the Gulf of Mexico. The density model contains the water and salt bodies present in the velocity model but also contains discrete layers in the sediments that serve to produce the desired reflec-

tion events. The use of both a velocity and density model makes it possible to adjust the reflectivity so that the relative amplitudes of primaries and multiples mimic those observed on real data. The velocity and density models constructed for the Atlantis structure are 40 km wide in the x -direction, 42.1 km wide in the y -direction, 10 km deep, and have a 25-m grid size in x , y , and z . This grid size supports a frequency band of approximately 2 to 15 Hz. A cropped depth slice and two orthogonal cross sections through the density model are shown in Figure 2. All future images in this paper are cropped to this same size. The dashed gold lines show the positions of the cross sections and depth slice. The red box drawn inside the depth slice shown in Figure 2 is 25×25 km. It encloses the shots for the towed-streamer data. The shot interval is 250 m in both the x - and y -directions. This yields 10,000 shots for the free-surface case and another 10,000 shots for the absorbing-surface case. The 10×15 km gold-colored box represents the outline of the originally planned OBS survey, whereas the 17×21 km blue box gives the outline of the 5727 OBS-node locations modeled for each of the following cases: absorbing-surface p only, free-surface p , and free-surface z . The receiver grid recorded for each shot is 16×16 km, is centered on the shot, and has a 50-m group interval in both the x - and y -directions. All data images shown here are extracted from 3D migrated volumes produced by common-shot migration using the exact velocity model and the $\omega - x$ extrapolation method mentioned earlier.

RESULTS

I extracted a NATS survey, oriented in the x -direction, from the free-surface, towed-streamer shots acquired over the Atlantis 3D model. Ten 8-km cables spaced 100 m apart were selected from the appropriate shot records. The sail-line separation was 500 m. No multiple suppression was applied before migration. (An image obtained without free-surface multiples is shown for comparison.) The only processing done before migration was a simple time-shift to center the causal wavelet on reflection events.

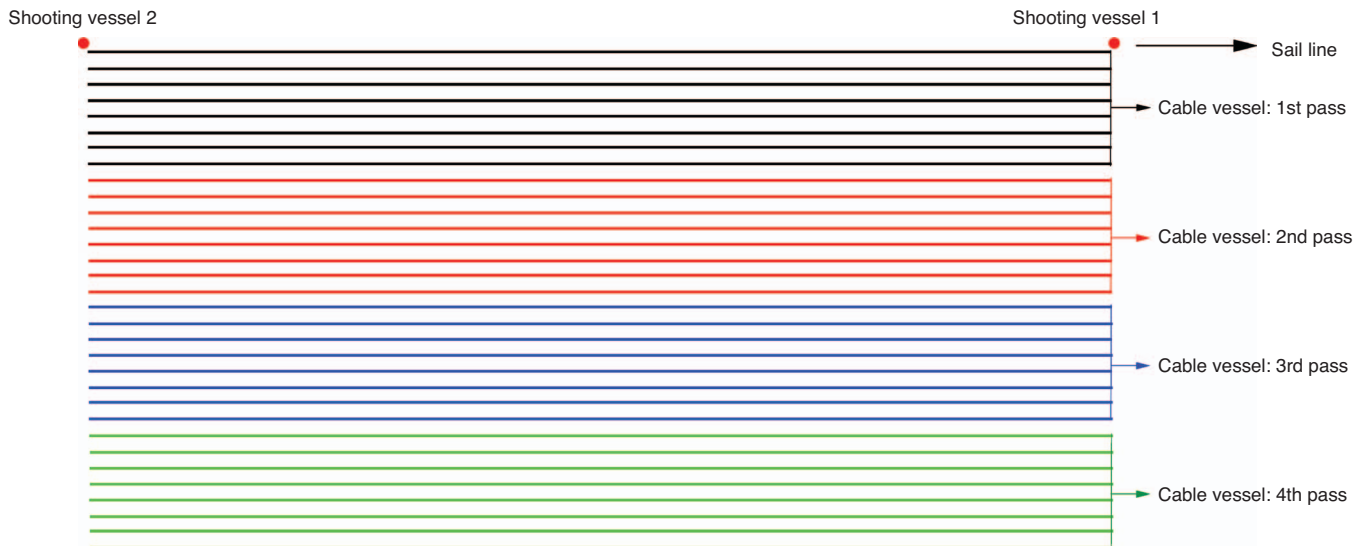


Figure 1. Implementation of the WATS method used by BP at Mad Dog. The cable vessel pulled eight 8-km cables spaced 125 m apart. Two source vessels were positioned as indicated. Four passes, called tiles, were used to achieve the desired 4-km width. The sail-line separation was 250 m.

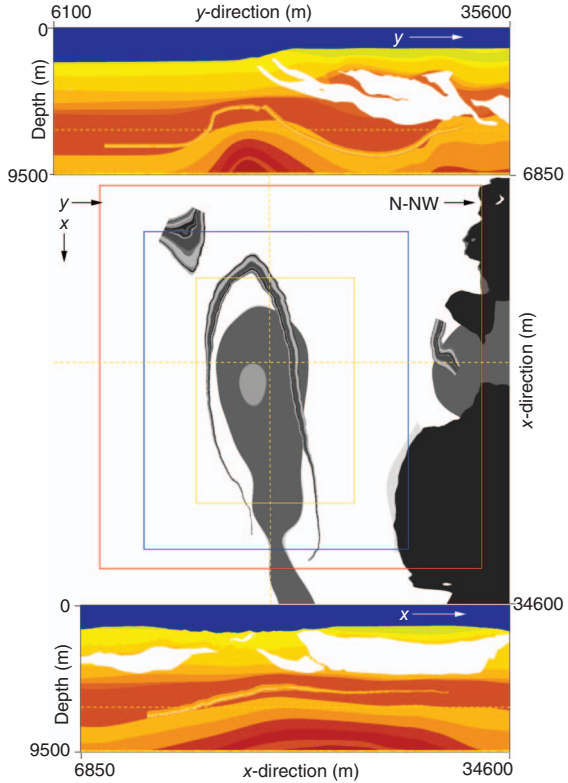


Figure 2. Cross sections and depth slice through the Atlantis 3D density model.

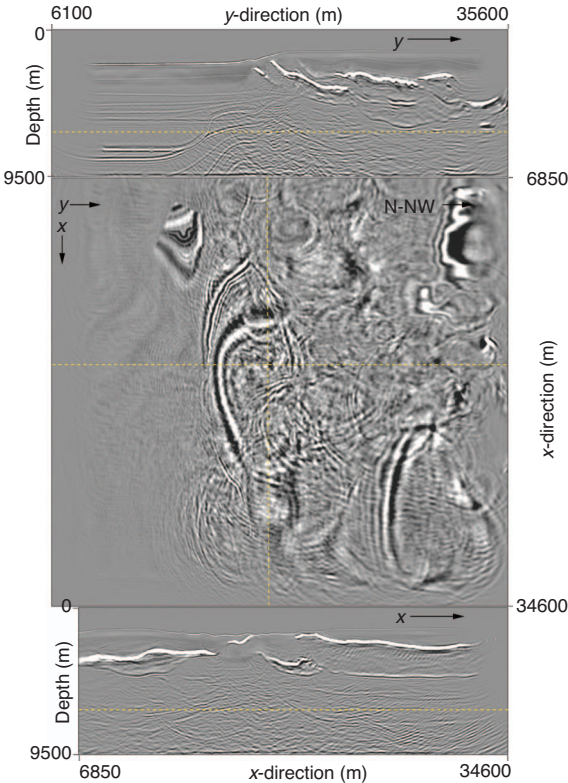


Figure 3. Prestack depth migration (PSDM) of free-surface FD data for a NATS survey oriented in the x -direction. No multiple suppression has been applied in processing.

The resulting prestack depth migration is shown in Figure 3. We cannot attribute the poor image quality to velocity error because the exact velocity model is used in imaging. If the problem is mostly illumination, one solution that has often been suggested is to acquire a number of NATS surveys at different azimuths to form a multiazimuth towed-streamer (MATS) survey. Figure 4 shows the prestack depth-migrated image resulting from combining four NATS surveys with azimuths at 45° increments. Comparison of this MATS result with a single NATS survey shows an improvement. The MATS result has healed some of the illumination gaps present in the NATS image; however, the overall image quality is still poor. Let's consider next the effect of free-surface multiples on NATS image quality.

If a NATS geometry identical to that shown in Figure 3 is synthesized from the absorbing-surface data so that no free-surface multiples are present, we get the result shown in Figure 5. It is clear that the image quality is vastly improved over that of the free-surface case. This suggests that free-surface multiples are a major factor in the poor image quality of NATS subsalt surveys. However, the NATS image is still poor over important portions of the subsalt structure, and illumination gaps are still present. Thus, even if we could somehow accomplish a perfect removal of free-surface multiple energy, we still would fail to achieve adequate subsalt images.

There are several interesting questions relating to the MATS geometry that are beyond the scope of this paper. First, how effective will be conventional multiple-removal procedures, such as 3D surface-related-multiple elimination (SRME), be on the individual NATS surveys that comprise the MATS result? Second, would the imaging problems be solved if one could achieve sufficient free-surface multiple suppression? If so, how many NATS surveys would it

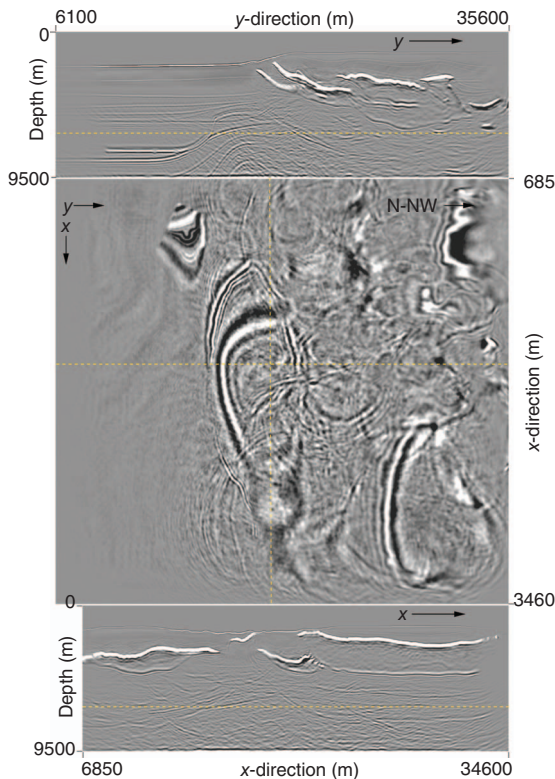


Figure 4. PSDM of free-surface FD data for a MATS survey consisting of the combination of four NATS surveys oriented at 45° increments.

take? Finally, could we find the correct velocity model by analyzing the individual NATS surveys that comprise the MATS result?

Our approach for subsalt imaging problems in the deepwater Gulf of Mexico is to record a receiver patch (for WATS data) or a source patch (for OBS-nodes) that contains a continuous and broad range of azimuths. Essentially, we seek to form a large antenna with as little leakage of undesired events as possible. Let's turn now to the WATS geometry and observe its effect on illumination gaps and multiple suppression.

I extract a WATS geometry similar to that shown in Figure 1 from the Atlantis 3D free-surface model data by selecting forty 8-km cables spaced 100 m apart, two sources located on the side of the receiver patch, and a 250-m sail-line separation. The prestack depth migration results are shown in Figure 6 for sail lines oriented in the *x*-direction and in Figure 7 for sail lines oriented in the *y*-direction. It is clear that the overall image quality is very good and is far superior to that present in the NATS and MATS images, even when the NATS image contains no free-surface multiples. Although no multiple suppression has been applied in processing before migration, it appears that most of the multiple energy has been eliminated. It is also apparent that the *x*- and *y*-oriented WATS surveys are equally good. Therefore, this WATS design is robust with regard to survey orientation.

The WATS result shown in Figure 7 can be improved by suppressing free-surface multiples before migration. Applying the wave-field-extrapolation method of Xia et al. (2006) yields the result shown in Figure 8. It is clear that many of the free-surface multiples remaining in the result shown in Figure 7 have been eliminated. For comparison, Figure 9 shows the migrated result for the same WATS geometry extracted from the absorbing-surface data. There are no

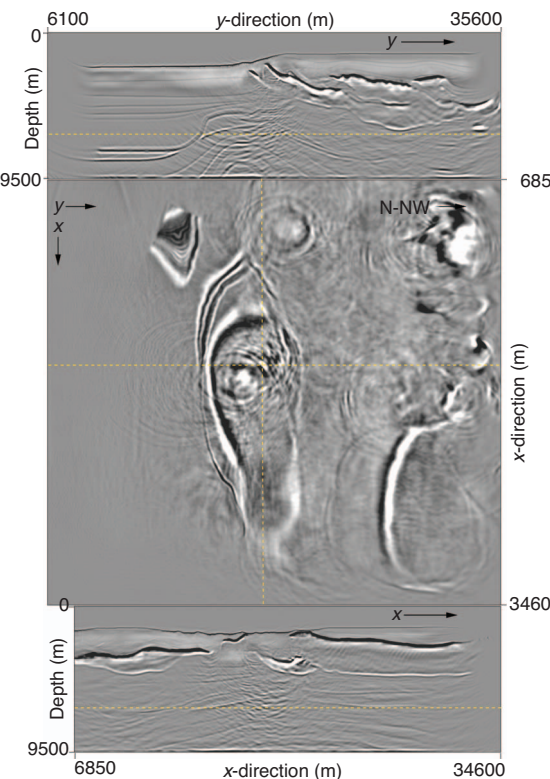


Figure 5. PSDM result for a NATS survey oriented in the *x*-direction. No free-surface multiples are present in the data.

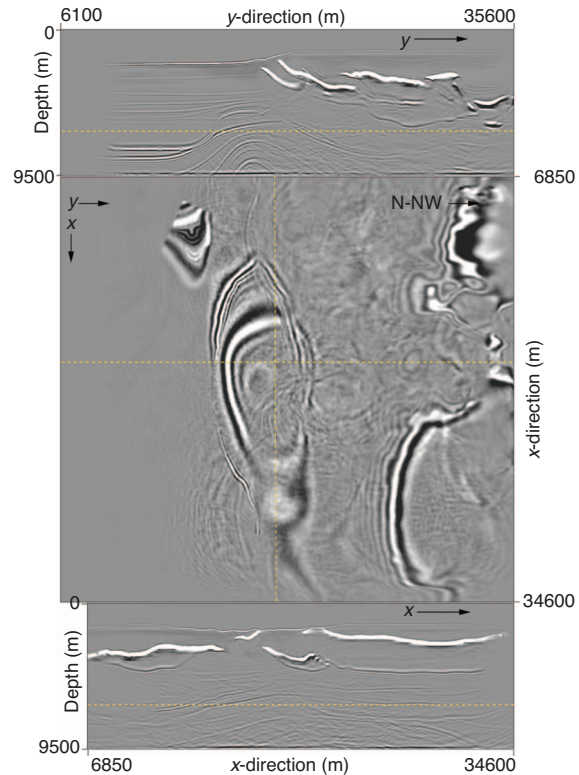


Figure 6. PSDM of free-surface FD data for a Mad Dog style WATS survey oriented in the *x*-direction.

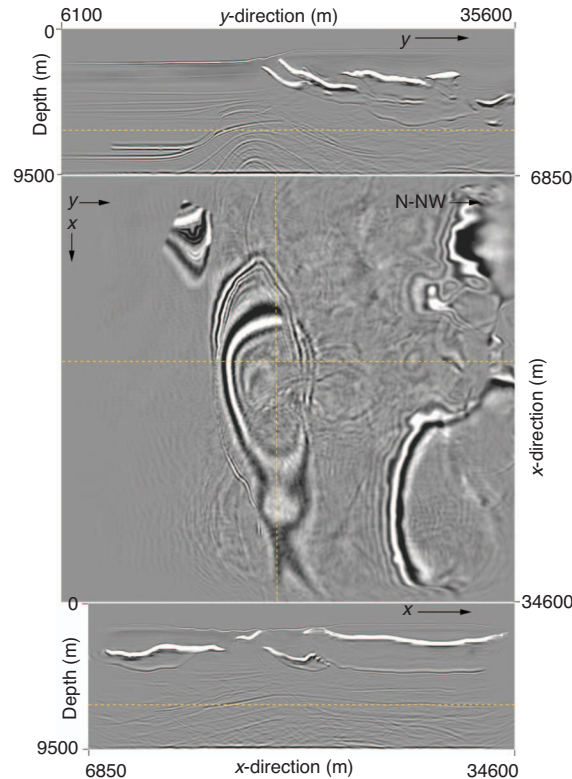


Figure 7. PSDM of free-surface FD data for a Mad Dog style WATS survey oriented in the *y*-direction.

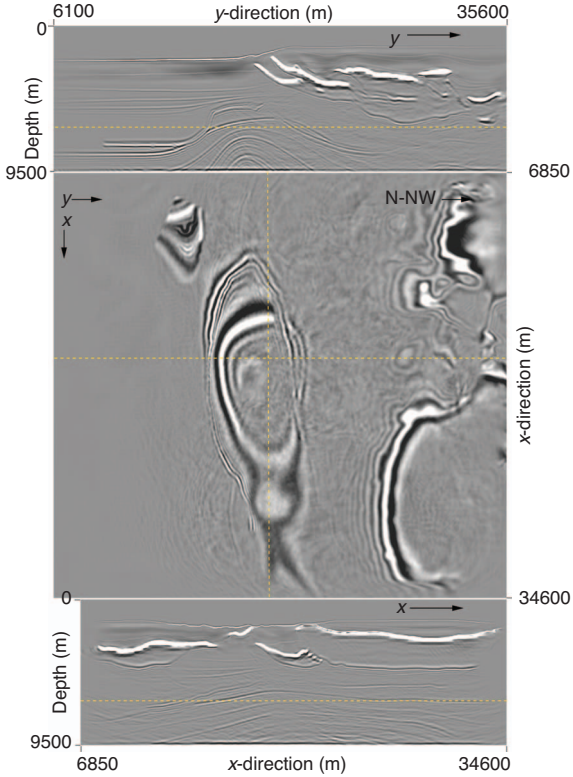


Figure 8. PSDM of free-surface FD data for a Mad Dog style WATS survey oriented in the y -direction after multiple suppression using a wavefield-extrapolation method.

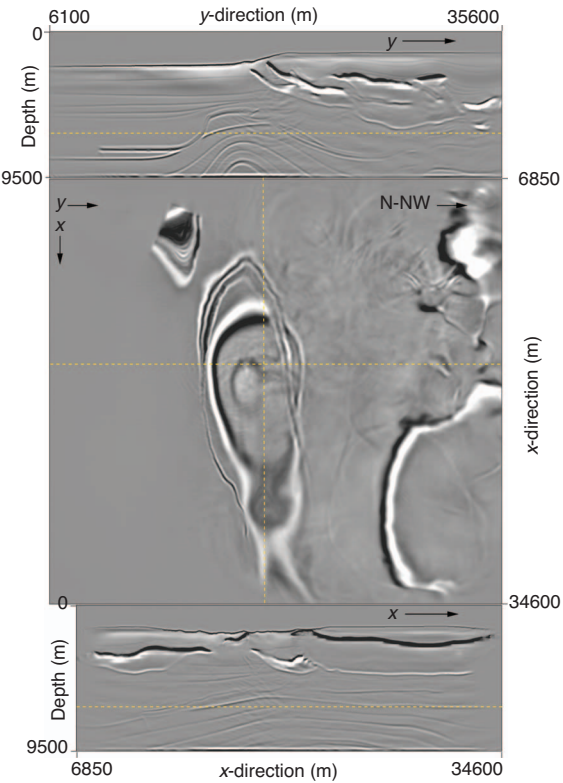


Figure 9. PSDM of absorbing-surface FD data for a Mad Dog style WATS survey oriented in the y -direction.

free-surface multiples in this result, and the image quality is only slightly better than that shown in Figure 8. Thus, the WATS geometry coupled with an effective multiple-suppression procedure in processing removes most of the free-surface multiple energy.

Two of the key parameters with the WATS design, receiver patch width and sail-line separation, may be varied to greatly reduce the cost of acquisition while still providing data quality superior to NATS methods. For example, if we reduce the receiver-patch width used in the WATS design shown in Figure 7 by a factor of two, and increase the sail-line separation to 500 m, we would reduce the acquisition cost by a factor of four, while still producing the image quality shown in Figure 10. Although not as good as that shown in Figure 7, this level of image quality may be well suited for exploration use. At BP, we refer to these more economical exploration-style WATS designs as XWATS. In 2006, many cable vessels could tow ten cables at 120-m spacings. Thus, a two-tile arrangement yields a receiver-patch width of 2400 m. With this receiver-patch width, the preferred sail-line separations needed to prevent fold striping are either 300 m or 600 m, with the latter preferred for exploration.

To simulate this geometry, I generated an additional 4100 shots over the Atlantis model using free-surface boundary conditions. The shot interval in each sail line remained 250 m and the sail-line separation was 600 m. I changed the group interval in each shot record to 30 m in both the x - and y -directions so that I could simulate 120-m cable spacings. The group interval within each cable was 30 m. The sail lines were oriented in the y -direction.

Figure 11 shows the result for this XWATS design. There are 20 cables spaced 120 m apart. The shots are on both ends of one side, as before, and the sail-line separation is 600 m. It is clear that the image

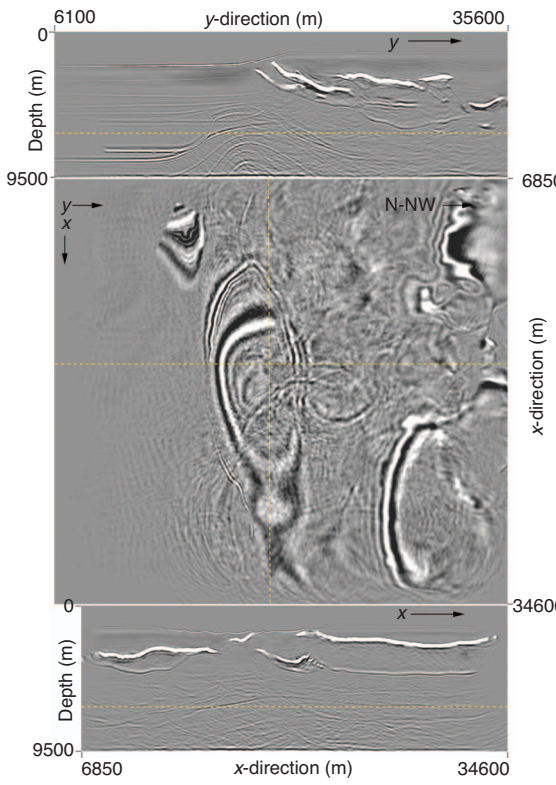


Figure 10. PSDM of free-surface FD data for a WATS survey oriented in the y -direction with an 8×2 km receiver patch and a 500-m sail-line separation.

quality has improved over that seen in Figure 10. The increase in receiver-patch width tends to improve image quality, whereas the increase in sail-line separation tends to decrease image quality. These results indicate that, although there has been a 20% increase in both, the receiver-patch width increase is more significant. Applying the wavefield-extrapolation multiple-suppression method discussed above to this geometry before migration yields the result shown in Figure 12. This result is quite good and rivals the image quality seen in the Mad Dog style WATS result seen in Figure 7 for less than one-quarter of the acquisition cost. Although this XWATS image quality isn't as good as that seen in Figure 8, it can easily be improved at any later time simply by adding more tiles and sail lines. The use of FD modeling plays a key role in optimizing these choices. Let's turn now to the OBS results.

Figure 13 shows the prestack depth migration result for the smaller OBS-node patch for P only and with no multiple suppression in processing (i.e., no P_z summation or wavefield extrapolation). The poor image quality is a result of several problems. First, there is much contamination by free-surface multiples. Second, the ghost reflection from the free surface is not part of the signal, as it is with towed-streamer data, but instead, it is strong multiple. Third, the size of the OBS-node patch is too small. The solution to these problems is to apply multiple suppression and to make the node patch larger. Figures 14 and 15 show the prestack depth migration results for the smaller and larger OBS-node patches, respectively, after suppressing multiples by applying P_z summation plus wavefield extrapolation before migration. The good result shown in Figure 15 suggests that the image quality obtained with wide-azimuth OBS methods is likely to be far better than that with NATS methods, that multiple

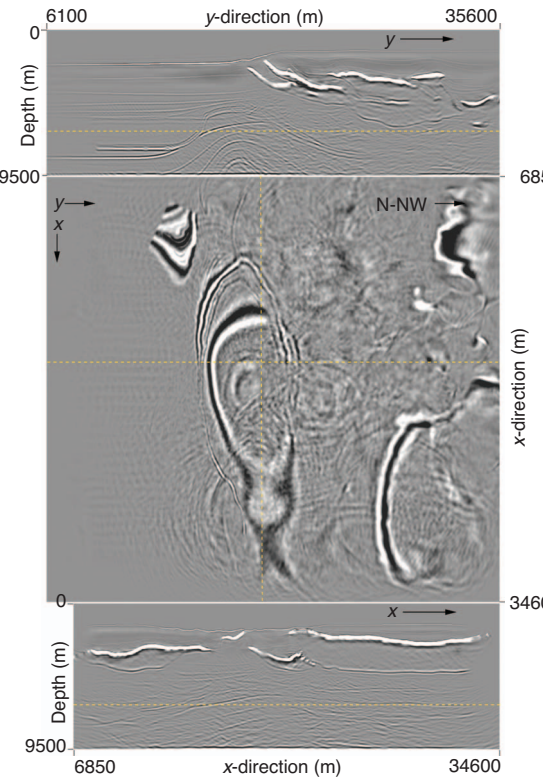


Figure 11. PSDM of free-surface FD data for a WATS survey oriented in the y -direction with an 8×2.4 km receiver patch and a 600-m sail-line separation.

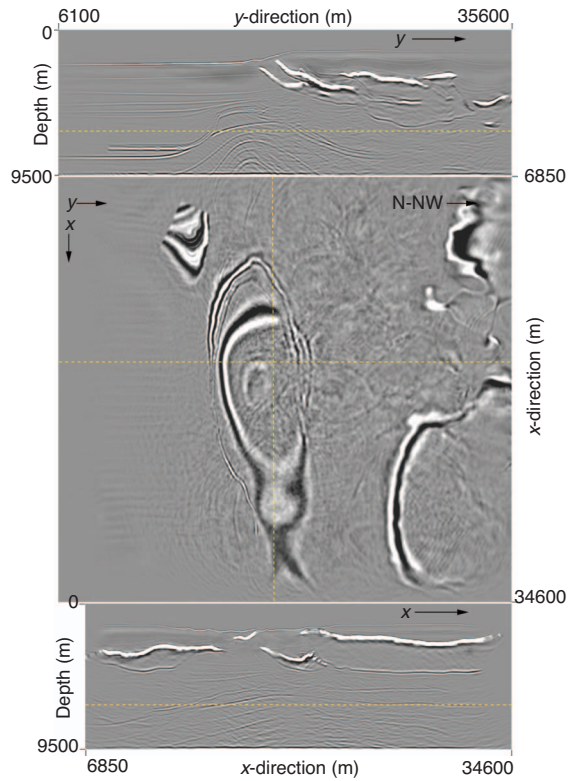


Figure 12. PSDM of free-surface FD data for a WATS survey oriented in the y -direction with an 8×2.4 km receiver patch and a 600-m sail-line separation after multiple suppression using a wavefield-extrapolation method.

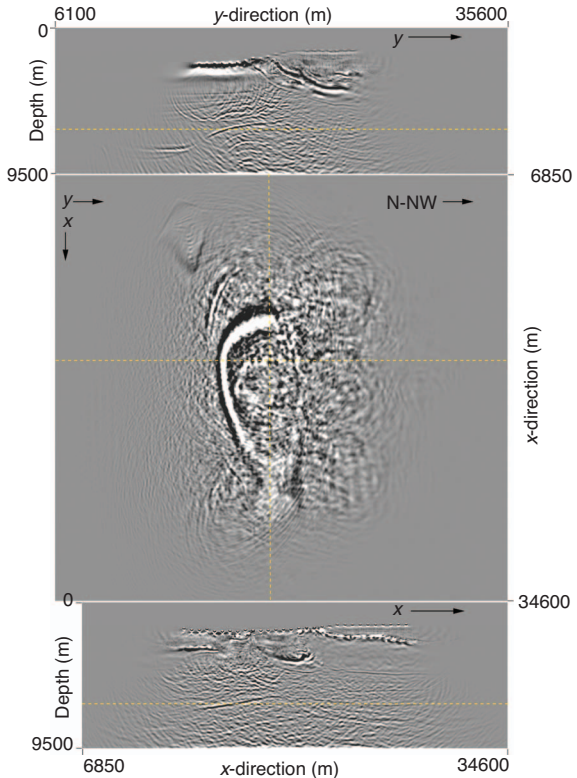


Figure 13. PSDM result for a 10×15 km OBS survey with a 500-m node spacing, P -component only, and no multiple suppression.

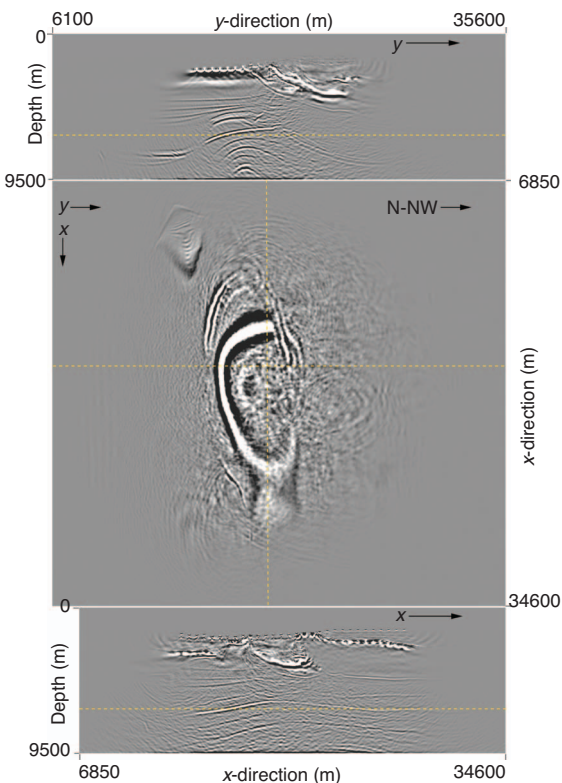


Figure 14. PSDM result for a 10×15 km OBS survey with a 500-m node spacing and PZ summation plus wavefield extrapolation for multiple suppression.

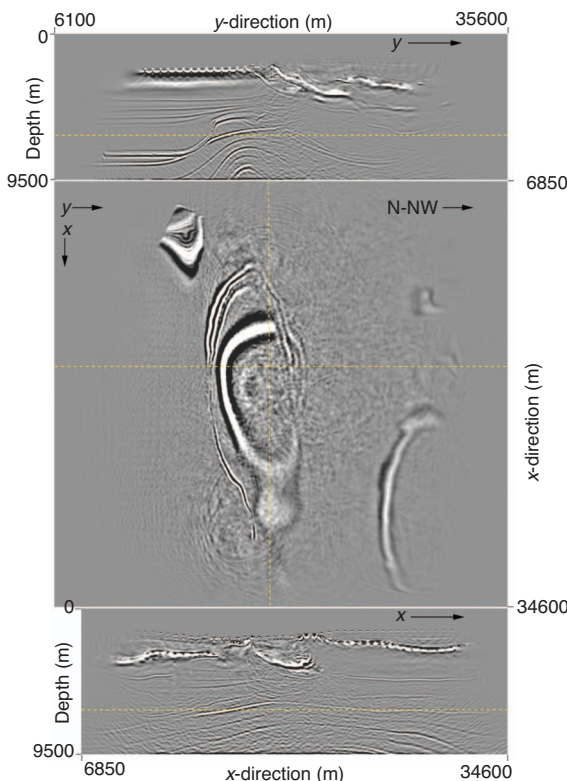


Figure 15. PSDM result for a 17×21 km OBS survey with a 500-m node spacing and PZ summation plus wavefield extrapolation for multiple suppression.

suppression with OBS surveys is crucial, and that small OBS surveys will not be satisfactory.

CONCLUSIONS

The described 3D FD modeling studies conducted for salt-related structures in the deepwater Gulf of Mexico demonstrate that NATS surveys created without free-surface multiples and imaged with exact velocity models yield greatly improved subsalt image quality when compared to those containing free-surface multiples. However, these NATS surveys without free-surface multiples still exhibit illumination problems and zones of poor data quality subsalt. Thus, it appears that both free-surface multiples and illumination are major factors in poor data quality subsalt. These modeling studies suggest that significant improvement in subsalt image quality may be obtained with wide-azimuth acquisition methods. These modeling studies also demonstrate that NATS surveys often fill the salt body with bogus reflection events, whereas the wide-azimuth surveys do not. This should yield a major advantage in velocity sensitivity to the wide-azimuth methods and permit one to come closer to achieving the correct velocity model. Two complementary wide-azimuth methods, OBS-nodes and WATS, can produce high-quality images suitable for field development. Furthermore, key parameters in the WATS method may be varied so that it may also be suitable for exploration use. An exploration-style WATS survey may be improved to that of appraisal and development quality at a later date merely by adding additional data as required. The cost for each method depends on structure-dependent parameters that may be optimized using 3D FD modeling.

ACKNOWLEDGMENTS

I thank John Etgen and Mike O'Brien for providing the imaging and modeling codes used in this study, Nurul Kabir for the multiple-removal processing on the OBS data, Ganyuan Xia for the multiple-removal processing on the WATS and XWATS data, BP's High Performance Computing team for the computer support, and BP for providing the tools and commitment needed to do this work and for permission to publish.

REFERENCES

- Amundsen, L., and A. Reitan, 1995, Decomposition of multi-component sea floor data into upgoing and downgoing P- and S-waves: *Geophysics*, **60**, 563–572.
- Barr, F., and J. Sanders, 1989, Attenuation of water-column reverberations using pressure and velocity detectors in a water-bottom cable: 59th Annual International Meeting, SEG, Expanded Abstracts, 653–656.
- Beaudoin, G., and S. Michell, 2006, The Atlantis OBS Project: OBS Nodes—defining the need, selecting the technology, and demonstrating the solution: Offshore Technology Conference, Paper OTC 17977.
- Claerbout, J., 1970, Coarse grid calculations of waves in inhomogeneous media with application to delineation of complex seismic structure: *Geophysics*, **35**, 407–418.
- , 1976, Fundamentals of geophysical data processing: McGraw-Hill Books Co.
- Clarke, R., G. Xia, N. Kabir, L. Sirgue, and S. Michell, 2006, Case study: A large 3D wide azimuth ocean bottom node survey in deepwater GOM: 76th Annual International Meeting, SEG, Expanded Abstracts, 1128–1132.
- Dablain, M., 1986, The application of high-order differencing to the scalar wave equation: *Geophysics*, **51**, 54–66.
- Etgen, J., and M. O'Brien, 2007, Computational methods for large-scale 3D finite-difference modeling: A tutorial: *Geophysics*, this issue.
- Etgen, J., and C. Regone, 1998, Strike shooting, dip shooting, widepatch shooting—Does prestack depth migration care? A model study: 68th An-

- nual International Meeting, SEG, Expanded Abstracts, 66–69.
- Holberg, O., 1987, Computational aspects of the choice of operator and sampling interval for numerical differentiation in large-scale simulation of wave phenomena: *Geophysical Prospecting*, **35**, 629–655.
- Igel, H., P. Mora, and B. Riollet, 1995, Anisotropic wave propagation through finite-difference grids: *Geophysics*, **60**, 1203–1216.
- Krail, P., 1994, Vertical cable as a subsalt imaging tool: *The Leading Edge*, **13**, 885–887.
- Michell, S., E. Shoshitaishvili, D. Chergotis, and J. Etgen, 2006, Wide azimuth streamer imaging of Mad Dog; Have we solved the subsalt imaging problem?: 76th Annual International Meeting, SEG, Expanded Abstracts, 2905–2909.
- Regone, C., 2006, A modeling approach to wide azimuth design for subsalt imaging: *The Leading Edge*, **12**, 1467–1475.
- Ross, A., and G. Beaudoin, 2006, Field design and operation of a deep water, wide azimuth node seismic survey, 76th Annual International Meeting, SEG, Expanded Abstracts, 2920–2924.
- Threadgold, I., K. Zembech-England, P. Gunnar Aas, P. Fontana, D. Hite, and W. Boone, 2006, Implementing a wide azimuth towed streamer field trial: The what, why and mostly how of WATS in Souther Green Canyon, 76th Annual International Meeting, SEG, Expanded Abstracts, 2901–2904.
- Virieux, J., 1986, P-SV wave propagation in heterogeneous media—Velocity stress method: *Geophysics*, **51**, 889–901.
- Xia, G., R. Clarke, J. Etgen, N. Kabir, K. Matson, and S. Michell, 2006, OBS multiple attenuation with application to the deepwater GOM Atlantis OBS nodes data: 76th Annual International Meeting, SEG, Expanded Abstracts, 2654–2658.